

Constraining gluon PDFs and TMDs with quarkonium production

Melih A. Ozelik

Institut de Physique Nucléaire Orsay/Université Paris-Sud

ozelik@ipno.in2p3.fr

Collaborators: M.G. Echevarria, J.-P. Lansberg, C. Pisano, A. Signori

DIS Torino

11 April 2019

the η_c - a good gluon probe

- η_c is a gluon probe at low scales

the η_c - a good gluon probe

- η_c is a gluon probe at low scales
- simplest of all quarkonia as far as computation of hadro-production

the η_c - a good gluon probe

- η_c is a gluon probe at low scales
- simplest of all quarkonia as far as computation of hadro-production
- η_c cross section computation known

the η_c - a good gluon probe

- η_c is a gluon probe at low scales
- simplest of all quarkonia as far as computation of hadro-production
- η_c cross section computation known
 - at NLO since 1992 in collinear factorisation

[J. Kühn, E. Mirkes, Phys.Lett. B296 (1992) 425-429]

the η_c - a good gluon probe

- η_c is a gluon probe at low scales
- simplest of all quarkonia as far as computation of hadro-production
- η_c cross section computation known
 - at NLO since 1992 in collinear factorisation

[J. Kühn, E. Mirkes, Phys.Lett. B296 (1992) 425-429]

- at LO since 2012 and at NLO since 2013 in TMD factorisation

[D. Boer, C. Pisano, Phys.Rev. D86 (2012) 094007]

[J.P. Ma, J.X. Wang, S. Zhao, Phys.Rev. D88 (2013) no.1, 014027]

the η_c - a good gluon probe

- η_c is a gluon probe at low scales
- simplest of all quarkonia as far as computation of hadro-production
- η_c cross section computation known
 - at NLO since 1992 in collinear factorisation

[J. Kühn, E. Mirkes, Phys.Lett. B296 (1992) 425-429]

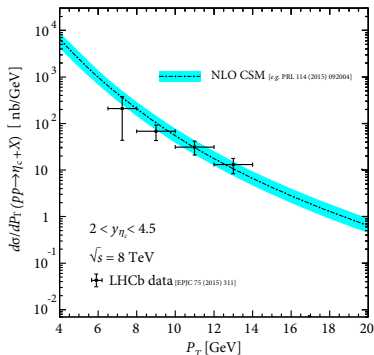
- at LO since 2012 and at NLO since 2013 in TMD factorisation

[D. Boer, C. Pisano, Phys.Rev. D86 (2012) 094007]

[J.P. Ma, J.X. Wang, S. Zhao, Phys.Rev. D88 (2013) no.1, 014027]

- first hadro-production measurement data released in 2015 by LHCb
($p_T > 6$ GeV)

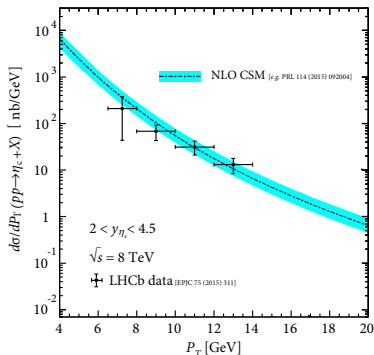
[LHCb, Eur.Phys.J. C75 (2015) no.7, 311.]



[M. Butenschoen, Z.-G. He, and B.A. Kniehl, PRL 114 (2015) 092004]

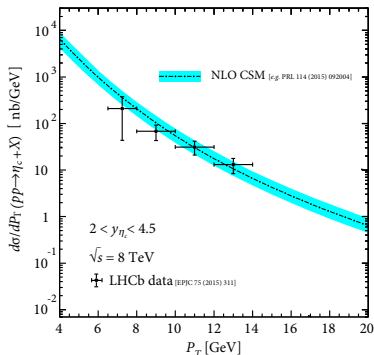
- first hadro-production measurement data released in 2014 by LHCb ($p_T > 6 \text{ GeV}$)

[LHCb, Eur.Phys.J. C 75 (2015) no.7, 311.]



[M. Butenschoen, Z.-G. He, and B.A. Kniehl, PRL 114 (2015) 092004]

- first hadro-production measurement data released in 2014 by LHCb ($p_T > 6$ GeV) [LHCb, Eur.Phys.J. C75 (2015) no.7, 311.]
 - NLO Colour-Singlet Model describes LHCb data well (see plot)



[M. Butenschoen, Z.-G. He, and B.A. Kniehl, PRL 114 (2015) 092004]

- first hadro-production measurement data released in 2014 by LHCb ($p_T > 6 \text{ GeV}$) [LHCb, Eur.Phys.J. C 75 (2015) no.7, 311.]
 - NLO Colour-Singlet Model describes LHCb data well (see plot)
 - unfortunately, data do not cover low p_T , however could be measured down to $p_T = 0$ at fixed-target experiment AFTER

[C. Hadjidakis et al., arXiv:1807.00603 [hep-ex]]

[Y. Feng et al., arXiv:1901.09766 [hep-ph]]

the η_c - a good gluon probe

- η_c is a gluon probe at low scales
- simplest of all quarkonia as far as computation of hadro-production
- η_c cross section computation known
 - at NLO since 1992 in collinear factorisation
 - at LO since 2012 and at NLO since 2013 in TMD factorisation
- first hadro-production measurement data released in 2014 by LHCb ($p_T > 6$ GeV)
 - NLO Colour-Singlet Model describes LHCb data well (see plot)
 - unfortunately, data do not cover low p_T , however could be measured down to $p_T = 0$ at fixed-target experiment AFTER
- encounter problem of *negative* cross-sections with η_c and other quarkonia bound states

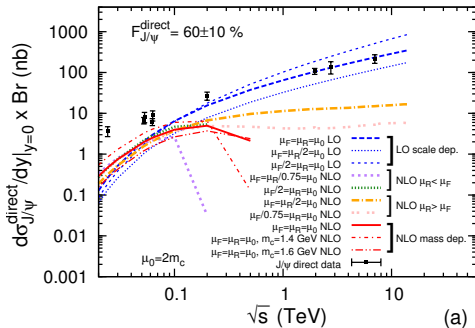
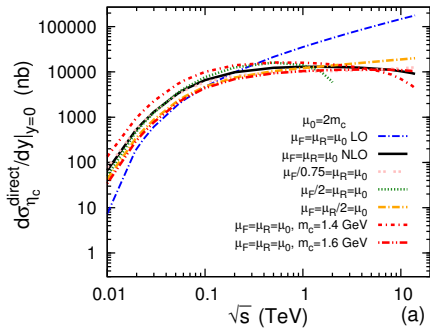
the η_c - a good gluon probe

- η_c is a gluon probe at low scales
- simplest of all quarkonia as far as computation of hadro-production
- η_c cross section computation known
 - at NLO since 1992 in collinear factorisation
 - at LO since 2012 and at NLO since 2013 in TMD factorisation
- first hadro-production measurement data released in 2014 by LHCb ($p_T > 6$ GeV)
 - NLO Colour-Singlet Model describes LHCb data well (see plot)
 - unfortunately, data do not cover low p_T , however could be measured down to $p_T = 0$ at fixed-target experiment AFTER
- encounter problem of *negative* cross-sections with η_c and other quarkonia bound states
- how to resolve the issue with *negative* cross-sections?

the η_c - a good gluon probe

- η_c is a gluon probe at low scales
- simplest of all quarkonia as far as computation of hadro-production
- η_c cross section computation known
 - at NLO since 1992 in collinear factorisation
 - at LO since 2012 and at NLO since 2013 in TMD factorisation
- first hadro-production measurement data released in 2014 by LHCb ($p_T > 6$ GeV)
 - NLO Colour-Singlet Model describes LHCb data well (see plot)
 - unfortunately, data do not cover low p_T , however could be measured down to $p_T = 0$ at fixed-target experiment AFTER
- encounter problem of *negative* cross-sections with η_c and other quarkonia bound states
- how to resolve the issue with *negative* cross-sections?
→ how is this related to PDFs and TMDs?

problem of negative cross-sections - η_c and J/ψ at NLO



comparison of η_c (left) and J/ψ (right) differential cross-sections at NLO with different scale choices of μ_R and μ_F with CTEQ6M

[Y. Feng, J.-P. Lansberg, J.X. Wang, Eur.Phys.J. C75 (2015) no.7, 313]

$$\mathcal{P}_{\text{physical}} = \sum_i \mathcal{P}_i \quad (1)$$

- physical probabilities $\mathcal{P}_{\text{physical}}$ are by definition positive

$$\mathcal{P}_{\text{physical}} = \sum_i \mathcal{P}_i \quad (1)$$

- physical probabilities $\mathcal{P}_{\text{physical}}$ are by definition positive
- sub-probabilities \mathcal{P}_i may be negative

$$\mathcal{P}_{\text{physical}} = \sum_i \mathcal{P}_i \quad (1)$$

- physical probabilities $\mathcal{P}_{\text{physical}}$ are by definition positive
- sub-probabilities \mathcal{P}_i may be negative
 - interpretation amounts to double-counting due to approximations/truncations; i.e. another prob. \mathcal{P}_j was too large hence needs to be subtracted

$$\mathcal{P}_{\text{physical}} = \sum_i \mathcal{P}_i \quad (1)$$

- physical probabilities $\mathcal{P}_{\text{physical}}$ are by definition positive
- sub-probabilities \mathcal{P}_i may be negative
 - interpretation amounts to double-counting due to approximations/truncations; i.e. another prob. \mathcal{P}_j was too large hence needs to be subtracted
 - example: Parton Distribution Functions can be negative for some x -values

$$\mathcal{P}_{\text{physical}} = \sum_i \mathcal{P}_i \quad (1)$$

- physical probabilities $\mathcal{P}_{\text{physical}}$ are by definition positive
- sub-probabilities \mathcal{P}_i may be negative
 - interpretation amounts to double-counting due to approximations/truncations; i.e. another prob. \mathcal{P}_j was too large hence needs to be subtracted
 - example: Parton Distribution Functions can be negative for some x -values
- *cross-sections* are *observable* quantities, hence physical probabilities $\mathcal{P}_{\text{physical}} (\sigma, \frac{d\sigma}{dy}, \dots)$ must be **positive**

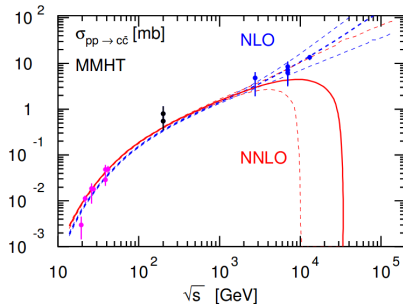
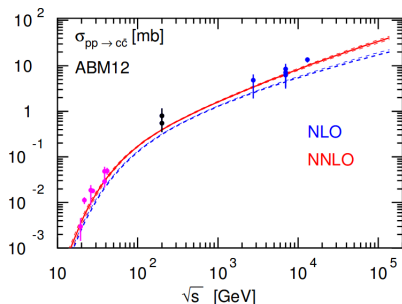
- What are potential sources for negative cross-sections?:

- What are potential sources for negative cross-sections?:
 - is it due to failure of theoretical models (NRQCD etc.) for quarkonia?

- What are potential sources for negative cross-sections?:
 - is it due to failure of theoretical models (NRQCD etc.) for quarkonia?
 - is it due to truncation of fixed-order calculation? Do we need to go to higher orders (N2LO, N3LO, ...) to solve the issue of negative cross-sections?

- What are potential sources for negative cross-sections?:
 - is it due to failure of theoretical models (NRQCD etc.) for quarkonia?
 - is it due to truncation of fixed-order calculation? Do we need to go to higher orders (N2LO, N3LO, ...) to solve the issue of negative cross-sections?
 - is it due to collinear factorisation? Do we need to include TMD effects?

negative cross-sections - open $c\bar{c}$ production at N2LO

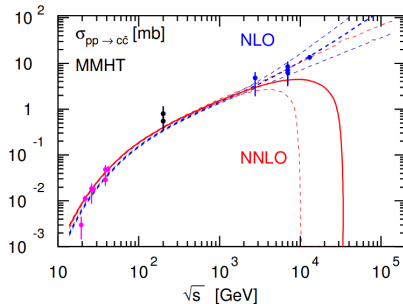
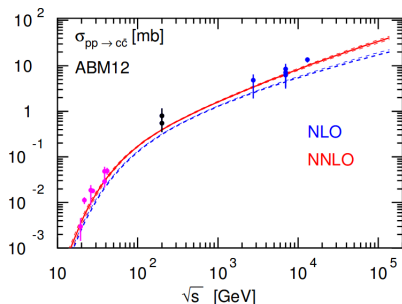


open $c\bar{c}$ production at NLO/N2LO, comparison with different PDFs (ABM12, MMHT)

[Accardi et al., Eur.Phys.J. C76 (2016) no.8, 471]

in this case, people attribute the negative cross-section to negative gluon PDFs at low scales and rather low- x , however

negative cross-sections - open $c\bar{c}$ production at N2LO



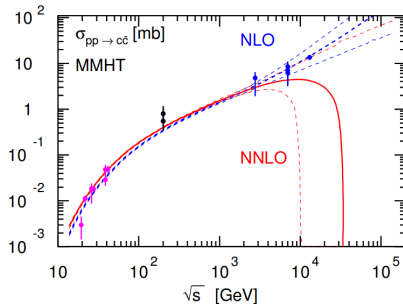
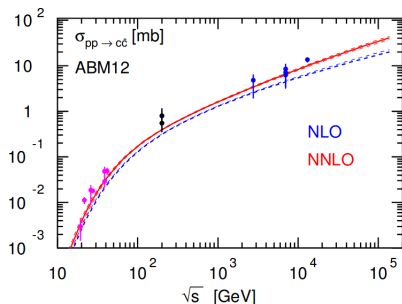
open $c\bar{c}$ production at NLO/N2LO, comparison with different PDFs (ABM12, MMHT)

[Accardi et al., Eur.Phys.J. C76 (2016) no.8, 471]

in this case, people attribute the negative cross-section to negative gluon PDFs at low scales and rather low- x , however

- $\frac{d\sigma}{dy}$ does not exist at NNLO

negative cross-sections - open $c\bar{c}$ production at N2LO



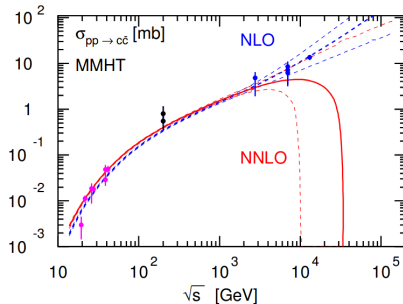
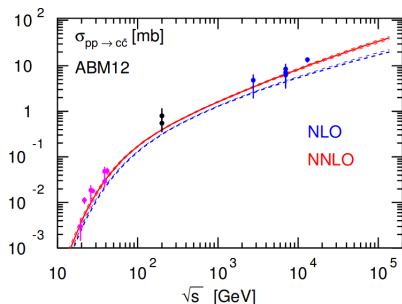
open $c\bar{c}$ production at NLO/N2LO, comparison with different PDFs (ABM12, MMHT)

[Accardi et al., Eur.Phys.J. C76 (2016) no.8, 471]

in this case, people attribute the negative cross-section to negative gluon PDFs at low scales and rather low- x , however

- $\frac{d\sigma}{dy}$ does not exist at NNLO
- full scale analysis not yet performed

negative cross-sections - open $c\bar{c}$ production at N2LO



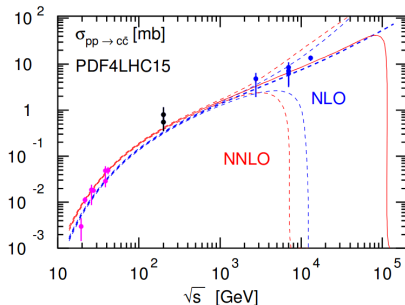
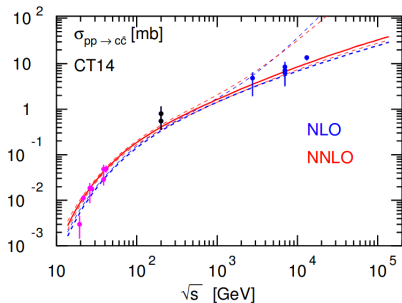
open $c\bar{c}$ production at NLO/N2LO, comparison with different PDFs (ABM12, MMHT)

[Accardi et al., Eur.Phys.J. C76 (2016) no.8, 471]

in this case, people attribute the negative cross-section to negative gluon PDFs at low scales and rather low- x , however

- $\frac{d\sigma}{dy}$ does not exist at NNLO
- full scale analysis not yet performed
→ therefore one cannot rule out the possibility of negative cross-sections with positive PDFs

negative cross-sections - open $c\bar{c}$ production at N2LO



open $c\bar{c}$ production at NLO/N2LO, comparison with different PDFs
(CT14, PDF4LHC15)

[Accardi et al., Eur.Phys.J. C76 (2016) no.8, 471]

- What are potential sources for negative cross-sections?:
 - ~~is it due to failure of theoretical models (NRQCD etc.) for quarkonia?~~
→ No, it is a more general problem; see open $c\bar{c}$ production
 - ~~is it due to truncation of fixed order calculation? Do we need to go to higher orders (N2LO, N3LO, ...) to solve the issue of negative cross-sections?~~ → No, the situation at higher orders will be worse; see open $c\bar{c}$ production
 - is it due to collinear factorisation? Do we need to include TMD effects?

- What are potential sources for negative cross-sections?:
 - ~~is it due to failure of theoretical models (NRQCD etc.) for quarkonia?~~
→ No, it is a more general problem; see open $c\bar{c}$ production
 - ~~is it due to truncation of fixed order calculation? Do we need to go to higher orders (N2LO, N3LO, ...) to solve the issue of negative cross-sections?~~ → No, the situation at higher orders will be worse; see open $c\bar{c}$ production
 - is it due to collinear factorisation? Do we need to include TMD effects? (see TMD side)
 - is it due to improper choices of renormalisation μ_R and factorisation μ_F scales?

- What are potential sources for negative cross-sections?:
 - ~~is it due to failure of theoretical models (NRQCD etc.) for quarkonia?~~
→ No, it is a more general problem; see open $c\bar{c}$ production
 - ~~is it due to truncation of fixed order calculation? Do we need to go to higher orders (N2LO, N3LO, ...) to solve the issue of negative cross-sections?~~ → No, the situation at higher orders will be worse; see open $c\bar{c}$ production
 - is it due to collinear factorisation? Do we need to include TMD effects? (see TMD side)
 - is it due to improper choices of renormalisation μ_R and factorisation μ_F scales?
 - or is it due to Parton Distribution Functions (PDFs)?

collinear factorisation - η_c at NLO - hadronic cross-section

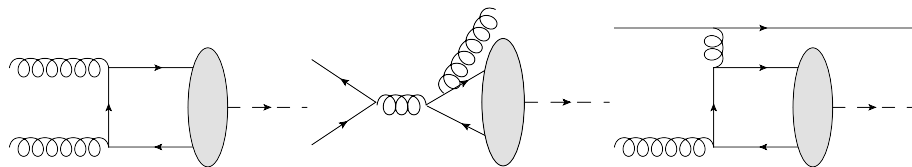
process

$$p + p \rightarrow \eta_c + X \quad (2)$$

hadronic cross-section

$$\sigma_{pp} = \sum_{ij} \int dx_1 dx_2 f_{i/p}(x_1, \mu_F) f_{j/p}(x_2, \mu_F) \hat{\sigma}_{ij}(\mu_R, \mu_F, x_1, x_2, \hat{S} = s x_1 x_2) \quad (3)$$

hadronic cross-section has dependence on the scales (μ_R, μ_F, s)



three channels contributing to η_c production at NLO; left - gg channel, middle - $q\bar{q}$ channel, right - qg channel

- J. Kühn & E. Mirkes compute pseudo-scalar toponium cross-section at NLO in 1992

[J. Kühn, E. Mirkes, Phys.Lett. B296 (1992) 425-429]

- J. Kühn & E. Mirkes compute pseudo-scalar toponium cross-section at NLO in 1992 [J. Kühn, E. Mirkes, Phys.Lett. B296 (1992) 425-429]
- G. Schuler publishes his Review in 1994 [G. Schuler, arXiv:hep-ph/9403387]

- J. Kühn & E. Mirkes compute pseudo-scalar toponium cross-section at NLO in 1992 [J. Kühn, E. Mirkes, Phys.Lett. B296 (1992) 425-429]
- G. Schuler publishes his Review in 1994 [G. Schuler, arXiv:hep-ph/9403387]
 - confirms result by J. Kühn & E. Mirkes

- J. Kühn & E. Mirkes compute pseudo-scalar toponium cross-section at NLO in 1992 [J. Kühn, E. Mirkes, Phys.Lett. B296 (1992) 425-429]
- G. Schuler publishes his Review in 1994 [G. Schuler, arXiv:hep-ph/9403387]
 - confirms result by J. Kühn & E. Mirkes
 - points out issues with negative cross-sections at high energies

- J. Kühn & E. Mirkes compute pseudo-scalar toponium cross-section at NLO in 1992 [J. Kühn, E. Mirkes, Phys.Lett. B296 (1992) 425-429]
- G. Schuler publishes his Review in 1994 [G. Schuler, arXiv:hep-ph/9403387]
 - confirms result by J. Kühn & E. Mirkes
 - points out issues with negative cross-sections at high energies
 - demonstrates that for some PDF choices there is strong/weak scale dependence

- J. Kühn & E. Mirkes compute pseudo-scalar toponium cross-section at NLO in 1992 [J. Kühn, E. Mirkes, *Phys.Lett.* B296 (1992) 425-429]
- G. Schuler publishes his Review in 1994 [G. Schuler, arXiv:hep-ph/9403387]
 - confirms result by J. Kühn & E. Mirkes
 - points out issues with negative cross-sections at high energies
 - demonstrates that for some PDF choices there is strong/weak scale dependence
- M. Mangano comes to same conclusions as G. Schuler in his 1996 Proceedings [M.L. Mangano, A. Petrelli, *Int.J.Mod.Phys.* A12 (1997) 3887-3897]

- J. Kühn & E. Mirkes compute pseudo-scalar toponium cross-section at NLO in 1992 [J. Kühn, E. Mirkes, Phys.Lett. B296 (1992) 425-429]
- G. Schuler publishes his Review in 1994 [G. Schuler, arXiv:hep-ph/9403387]
 - confirms result by J. Kühn & E. Mirkes
 - points out issues with negative cross-sections at high energies
 - demonstrates that for some PDF choices there is strong/weak scale dependence
- M. Mangano comes to same conclusions as G. Schuler in his 1996 Proceedings [M.L. Mangano, A. Petrelli, Int.J.Mod.Phys. A12 (1997) 3887-3897]
- A. Petrelli *et al.* confirm result by J. Kühn & E. Mirkes in 1997 [A. Petrelli et al., Nucl.Phys. B514 (1998) 245-309]

- J. Kühn & E. Mirkes compute pseudo-scalar toponium cross-section at NLO in 1992 [J. Kühn, E. Mirkes, Phys.Lett. B296 (1992) 425-429]
- G. Schuler publishes his Review in 1994 [G. Schuler, arXiv:hep-ph/9403387]
 - confirms result by J. Kühn & E. Mirkes
 - points out issues with negative cross-sections at high energies
 - demonstrates that for some PDF choices there is strong/weak scale dependence
- M. Mangano comes to same conclusions as G. Schuler in his 1996 Proceedings [M.L. Mangano, A. Petrelli, Int.J.Mod.Phys. A12 (1997) 3887-3897]
- A. Petrelli *et al.* confirm result by J. Kühn & E. Mirkes in 1997 [A. Petrelli et al., Nucl.Phys. B514 (1998) 245-309]
- I confirm that everybody above was correct ;-)

- appearance of negative cross-sections for quarkonia at high energies

- appearance of negative cross-sections for quarkonia at high energies
- Schuler identifies two potential sources

- appearance of negative cross-sections for quarkonia at high energies
- Schuler identifies two potential sources
 - small x -behaviour of gluon and sea-quark distributions

- appearance of negative cross-sections for quarkonia at high energies
- Schuler identifies two potential sources
 - small x -behaviour of gluon and sea-quark distributions
 - behaviour of partonic cross-sections away from threshold

¶Most of the remarks which follow have already been made by G. Schuler in his '94 review [9]. Schuler at the time had available the full NLO corrections to η production, as well as the leading small- x behaviour of the χ cross sections. It is a pity that those remarks have passed almost unnoticed in the community!

[M.L. Mangano, A. Petrelli, *Int.J.Mod.Phys. A12 (1997) 3887-3897*]

¶Most of the remarks which follow have already been made by G. Schuler in his '94 review [9]. Schuler at the time had available the full NLO corrections to η production, as well as the leading small- x behaviour of the χ cross sections. It is a pity that those remarks have passed almost unnoticed in the community!

[M.L. Mangano, A. Petrelli, *Int.J.Mod.Phys. A12 (1997) 3887-3897*]

- arrives to similar conclusions that steeper gluon PDF choices will give better results because real corrections become less relevant (see Schuler's table) at high hadronic energies

¶Most of the remarks which follow have already been made by G. Schuler in his '94 review [9]. Schuler at the time had available the full NLO corrections to η production, as well as the leading small- x behaviour of the χ cross sections. It is a pity that those remarks have passed almost unnoticed in the community!

[M.L. Mangano, A. Petrelli, *Int.J.Mod.Phys. A12 (1997) 3887-3897*]

- arrives to similar conclusions that steeper gluon PDF choices will give better results because real corrections become less relevant (see Schuler's table) at high hadronic energies
- confirms that partonic limit away from threshold has the general structure,

$$\lim_{z \rightarrow 0} \hat{\sigma}_{gg} = 2C_A \frac{\alpha_s}{\pi} \hat{\sigma}_{\text{Born}} \left(\log \frac{M^2}{\mu_F^2} - C_J \right), \quad (4)$$

$$\lim_{z \rightarrow 0} \hat{\sigma}_{qg} = C_F \frac{\alpha_s}{\pi} \hat{\sigma}_{\text{Born}} \left(\log \frac{M^2}{\mu_F^2} - C_J \right), \quad (5)$$

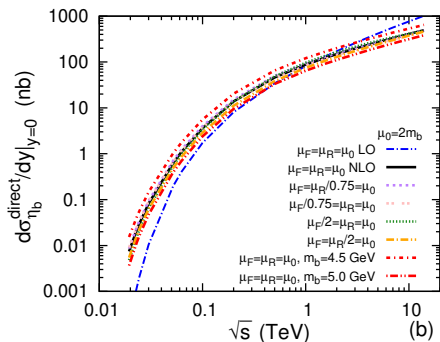
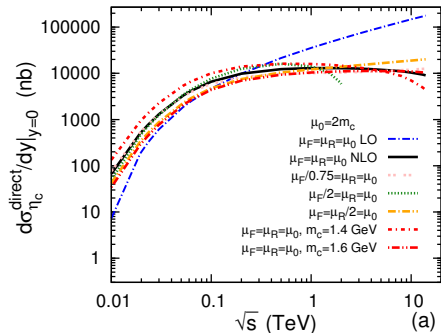
where C_J is a process-dependent quantity

- default scale choice is $\mu_R = \mu_F = 2m_c = 3\text{GeV}$

- default scale choice is $\mu_R = \mu_F = 2m_c = 3\text{GeV}$
- most PDFs are parametrised at a scale close to the mass of the charm quark meaning that the PDFs will strongly depend on the input of the initial parametrisation, hence no sufficient evolution of DGLAP equations

[M.L. Mangano, A. Petrelli, *Int.J.Mod.Phys. A12* (1997) 3887-3897]

- default scale choice is $\mu_R = \mu_F = 2m_c = 3\text{GeV}$
- most PDFs are parametrised at a scale close to the mass of the charm quark meaning that the PDFs will strongly depend on the input of the initial parametrisation, hence no sufficient evolution of DGLAP equations
[M.L. Mangano, A. Petrelli, Int.J.Mod.Phys. A12 (1997) 3887-3897]
- let's make a comparison with η_b , why do we not encounter negative cross-sections?



comparison of η_b differential cross-section at NLO with different choices of μ_R and μ_F with CTEQ6M

[Y. Feng, J.-P. Lansberg, J.X. Wang, Eur.Phys.J. C75 (2015) no.7, 313]

- η_b differential cross-section is much more stable than in case of η_c . The NLO result is the same for both particles. With only the mass increasing from m_c to m_b , we can describe three effects:

- η_b differential cross-section is much more stable than in case of η_c . The NLO result is the same for both particles. With only the mass increasing from m_c to m_b , we can describe three effects:
 - the dependence of the cross-section on \sqrt{s} is now stretched out by the ratio the mass changed

- η_b differential cross-section is much more stable than in case of η_c . The NLO result is the same for both particles. With only the mass increasing from m_c to m_b , we can describe three effects:
 - the dependence of the cross-section on \sqrt{s} is now stretched out by the ratio the mass changed
 - the rescaling of strong coupling constant α_s ; higher scales mean lower coupling \rightarrow QCD corrections become weaker, hence the NLO cross-section will be closer to LO

- η_b differential cross-section is much more stable than in case of η_c . The NLO result is the same for both particles. With only the mass increasing from m_c to m_b , we can describe three effects:
 - the dependence of the cross-section on \sqrt{s} is now stretched out by the ratio the mass changed
 - the rescaling of strong coupling constant α_s ; higher scales mean lower coupling \rightarrow QCD corrections become weaker, hence the NLO cross-section will be closer to LO
 - the third effect is evolution of the PDFs from the scale of η_c to η_b . Evolution leads to steeper gluon PDFs, hence real corrections are further suppressed

- η_b differential cross-section is much more stable than in case of η_c . The NLO result is the same for both particles. With only the mass increasing from m_c to m_b , we can describe three effects:
 - the dependence of the cross-section on \sqrt{s} is now stretched out by the ratio the mass changed
 - the rescaling of strong coupling constant α_s ; higher scales mean lower coupling \rightarrow QCD corrections become weaker, hence the NLO cross-section will be closer to LO
 - the third effect is evolution of the PDFs from the scale of η_c to η_b . Evolution leads to steeper gluon PDFs, hence real corrections are further suppressed
 \rightarrow **essentially ensuring the positivity of the η_b cross-section**

- η_b differential cross-section is much more stable than in case of η_c . The NLO result is the same for both particles. With only the mass increasing from m_c to m_b , we can describe three effects:
 - the dependence of the cross-section on \sqrt{s} is now stretched out by the ratio the mass changed
 - the rescaling of strong coupling constant α_s ; higher scales mean lower coupling \rightarrow QCD corrections become weaker, hence the NLO cross-section will be closer to LO
 - the third effect is evolution of the PDFs from the scale of η_c to η_b . Evolution leads to steeper gluon PDFs, hence real corrections are further suppressed
 - \rightarrow **essentially ensuring the positivity of the η_b cross-section**
 - note however that the NLO result start to deviate from LO at large \sqrt{s}

- What are potential sources for negative cross-sections?:
 - ~~is it due to failure of theoretical models (NRQCD etc.) for quarkonia?~~
→ No, it is a more general problem; see open $c\bar{c}$ production
 - ~~is it due to truncation of fixed order calculation? Do we need to go to higher orders (N2LO, N3LO, ...) to solve the issue of negative cross-sections?~~ → No, the situation at higher orders will be worse; see open $c\bar{c}$ production
 - do we even need to include k_T -Resummation? (see TMD side)
 - ~~is it due to bad choices of renormalisation μ_R and factorisation μ_F scales?~~ → No, since the η_c is a low scale process, it depends crucially on the PDF parametrisation; no physical reason to go to artificially large scales
 - or is it due to Parton Distribution Functions (PDFs)?

- What are potential sources for negative cross-sections?:
 - ~~is it due to failure of theoretical models (NRQCD etc.) for quarkonia?~~
→ No, it is a more general problem; see open $c\bar{c}$ production
 - ~~is it due to truncation of fixed order calculation? Do we need to go to higher orders (N2LO, N3LO, ...) to solve the issue of negative cross-sections?~~ → No, the situation at higher orders will be worse; see open $c\bar{c}$ production
 - do we even need to include k_T -Resummation? (see TMD side)
 - ~~is it due to bad choices of renormalisation μ_R and factorisation μ_F scales?~~ → No, since the η_c is a low scale process, it depends crucially on the PDF parametrisation; no physical reason to go to artificially large scales
 - **or is it due to Parton Distribution Functions (PDFs)?**

PDF parametrisation

- as pointed out by Schuler and Mangano, different PDF parametrisations can give very different result

PDF parametrisation

- as pointed out by Schuler and Mangano, different PDF parametrisations can give very different result
- we will put this into practice and compute the K-factor for 5 different PDF choices at $y=0$. We will plot the energy-dependence of the K-factor for the PDFs:

PDF parametrisation

- as pointed out by Schuler and Mangano, different PDF parametrisations can give very different result
- we will put this into practice and compute the K-factor for 5 different PDF choices at $y=0$. We will plot the energy-dependence of the K-factor for the PDFs:
 - CT14nlo_NF3

- as pointed out by Schuler and Mangano, different PDF parametrisations can give very different result
- we will put this into practice and compute the K-factor for 5 different PDF choices at $y=0$. We will plot the energy-dependence of the K-factor for the PDFs:
 - CT14nlo_NF3
 - NNPDF31sx_nlo_as_0118

- as pointed out by Schuler and Mangano, different PDF parametrisations can give very different result
- we will put this into practice and compute the K-factor for 5 different PDF choices at $y=0$. We will plot the energy-dependence of the K-factor for the PDFs:
 - CT14nlo_NF3
 - NNPDF31sx_nlo_as_0118
 - NNPDF31sx_nlonllx_as_0118

- as pointed out by Schuler and Mangano, different PDF parametrisations can give very different result
- we will put this into practice and compute the K-factor for 5 different PDF choices at $y=0$. We will plot the energy-dependence of the K-factor for the PDFs:
 - CT14nlo_NF3
 - NNPDF31sx_nlo_as_0118
 - NNPDF31sx_nlonllx_as_0118
 - MRS(A')

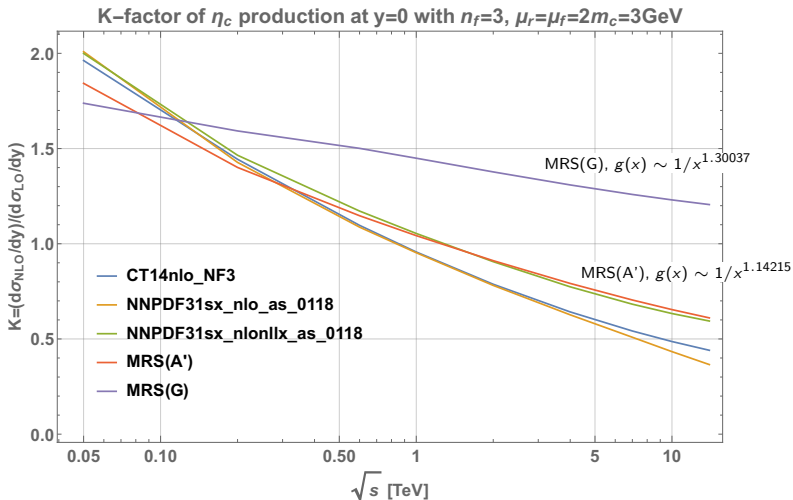
- as pointed out by Schuler and Mangano, different PDF parametrisations can give very different result
- we will put this into practice and compute the K-factor for 5 different PDF choices at $y=0$. We will plot the energy-dependence of the K-factor for the PDFs:
 - CT14nlo_NF3
 - NNPDF31sx_nlo_as_0118
 - NNPDF31sx_nlonllx_as_0118
 - MRS(A')
 - MRS(G)

- as pointed out by Schuler and Mangano, different PDF parametrisations can give very different result
- we will put this into practice and compute the K-factor for 5 different PDF choices at $y=0$. We will plot the energy-dependence of the K-factor for the PDFs:
 - CT14nlo_NF3
 - NNPDF31sx_nlo_as_0118
 - NNPDF31sx_nlonllx_as_0118
 - MRS(A')
 - MRS(G)
- in order to discriminate between the PDF choices we will use two different scale configurations:

- as pointed out by Schuler and Mangano, different PDF parametrisations can give very different result
- we will put this into practice and compute the K-factor for 5 different PDF choices at $y=0$. We will plot the energy-dependence of the K-factor for the PDFs:
 - CT14nlo_NF3
 - NNPDF31sx_nlo_as_0118
 - NNPDF31sx_nlonllx_as_0118
 - MRS(A')
 - MRS(G)
- in order to discriminate between the PDF choices we will use two different scale configurations:
 - $\mu_R = \mu_F = 2m_c = 3\text{GeV}$ - default scale choice

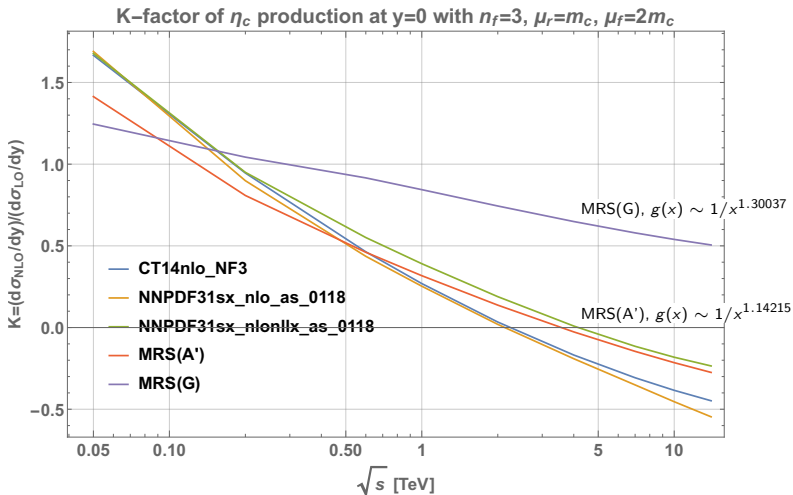
- as pointed out by Schuler and Mangano, different PDF parametrisations can give very different result
- we will put this into practice and compute the K-factor for 5 different PDF choices at $y=0$. We will plot the energy-dependence of the K-factor for the PDFs:
 - CT14nlo_NF3
 - NNPDF31sx_nlo_as_0118
 - NNPDF31sx_nlonllx_as_0118
 - MRS(A')
 - MRS(G)
- in order to discriminate between the PDF choices we will use two different scale configurations:
 - $\mu_R = \mu_F = 2m_c = 3\text{GeV}$ - default scale choice
 - $\mu_R = m_c = 1.5\text{GeV}$, $\mu_F = 2m_c = 3\text{GeV}$
 - lower renormalisation choice leads to larger $\alpha_s \rightarrow$ real emission contributions become more important; the objective is to see the impact of the PDFs on the real corrections

K-factor at $y = 0$ - $\mu_R = \mu_F = 2m_c = 3\text{GeV}$



K-factor at $y=0$ as a function of energy and with different PDF choices. Default scale choice used $\mu_R = \mu_F = 2m_c = 3\text{GeV}$.

K-factor at $y = 0$ - $\mu_R = m_c = 1.5\text{GeV}$, $\mu_F = 2m_c = 3\text{GeV}$



K-factor at $y=0$ as a function of energy and with different PDF choices.
Alternative scale choice used $\mu_R = m_c = 1.5\text{GeV}$, $\mu_F = 2m_c = 3\text{GeV}$.

Uncertainty of K -factor at $y = 0$ - 100 Replicas of NNP31_nlo_as_0118

- use standard NNP31_nlo_as_0118 set and run over 100 Replicas

Uncertainty of K -factor at $y = 0 - 100$ Replicas of NNPDF31_nlo_as_0118

- use standard NNPDF31_nlo_as_0118 set and run over 100 Replicas
- difference between NNPDF31_nlo_as_0118 and NNPDF31sx_nlo_as_0118 is that the latter one with small x extension has been probed at a minimally lower scale Q such that in the Replica generation the 2.7GeV^2 bin has been taken into account which turns out to be crucial

Uncertainty of K -factor at $y = 0 - 100$ Replicas of NNPDF31_nlo_as_0118

- use standard NNPDF31_nlo_as_0118 set and run over 100 Replicas
- difference between NNPDF31_nlo_as_0118 and NNPDF31sx_nlo_as_0118 is that the latter one with small x extension has been probed at a minimally lower scale Q such that in the Replica generation the 2.7GeV^2 bin has been taken into account which turns out to be crucial
- expect very large K -factor uncertainty associated to NNPDF31_nlo_as_0118 PDF choice

Uncertainty of K -factor at $y = 0 - 100$ Replicas of NNPDF31_nlo_as_0118

- use standard NNPDF31_nlo_as_0118 set and run over 100 Replicas
- difference between NNPDF31_nlo_as_0118 and NNPDF31sx_nlo_as_0118 is that the latter one with small x extension has been probed at a minimally lower scale Q such that in the Replica generation the 2.7GeV^2 bin has been taken into account which turns out to be crucial
- expect very large K -factor uncertainty associated to NNPDF31_nlo_as_0118 PDF choice
- we will try with two different scale choices as before, set $y = 0$ and use $\sqrt{s} = 115 \text{ GeV}, 7 \text{ TeV}$ and 14 TeV

K-factor results - $y = 0$ & $\sqrt{s} = 7$ TeV - 100 Replicas

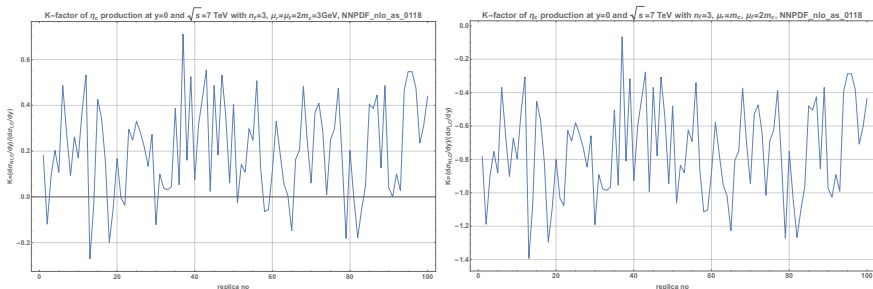


Figure: Strong variation of K -factor over replica number of NNPDF31_nlo_as_0118 ($y=0$, $\sqrt{s} = 7$ TeV, default/alternative scale choice)

default ($\mu_R = \mu_F = 2m_c = 3\text{GeV}$): $\rightarrow K = 0.2 \pm 0.2$

alternative ($\mu_R = m_c = 1.5\text{GeV}$, $\mu_F = 2m_c = 3\text{GeV}$): $\rightarrow K = -0.8 \pm 0.3$

K-factor results - $y = 0$ & $\sqrt{s} = 14$ TeV - 100 Replicas

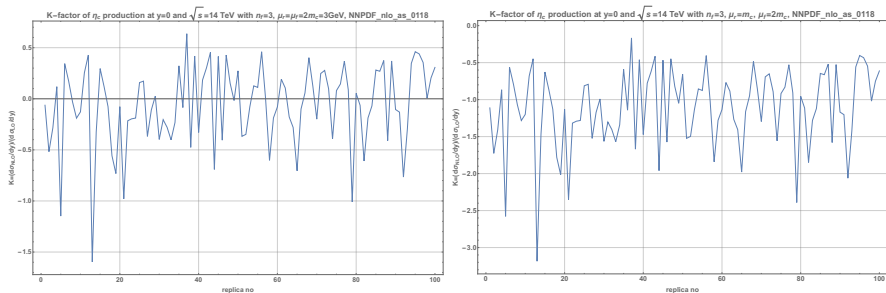


Figure: Strong variation of K -factor over replica number of NNPDF31_nlo_as_0118 ($y=0$, $\sqrt{s} = 14$ TeV, default/alternative scale choice)

default ($\mu_R = \mu_F = 2m_c = 3\text{GeV}$): $\rightarrow K = -0.1 \pm 0.4$

alternative ($\mu_R = m_c = 1.5\text{GeV}$, $\mu_F = 2m_c = 3\text{GeV}$): $\rightarrow K = -1.1 \pm 0.5$

K-factor - default scale - summary so far

	$\sqrt{s} = 7 \text{ TeV}$			$\sqrt{s} = 14 \text{ TeV}$
PDF choice	$y = 0$	$y = 1$	$y = 2$	$y = 0$
MRS(G)	1.26	1.27	1.29	1.21
MRS(A')	0.70	0.72	0.76	0.61
NNPDF31sx_nlonllx _as_0118	0.68	0.71	0.80	0.59
CT14nlo_NF3	0.54	0.57	0.65	0.44
NNPDF31sx_nlo _as_0118	0.51	0.52	0.61	0.37
NNPDF31_nlo _as_0118	0.2 ± 0.2	0.2 ± 0.4	0.2 ± 1.1	-0.1 ± 0.4

- can we improve the K -factor for NNPDF31_nlo_as_0118 PDF set by applying constraints?

Improve K -factor with constraints in Quarkonia

- can we improve the K -factor for NNPDF31_nlo_as_0118 PDF set by applying constraints?
- strategy is to discard all replicas that gave unphysical $d\sigma/dy < 0$ in a given set of results. We will assign weight 0 to each such replica

Improve K -factor with constraints in Quarkonia

- can we improve the K -factor for NNPDF31_nlo_as_0118 PDF set by applying constraints?
- strategy is to discard all replicas that gave unphysical $d\sigma/dy < 0$ in a given set of results. We will assign weight 0 to each such replica
- we will use the results for $y = 0$ and $\sqrt{s} = 14$ TeV with default scale choice

Improve K -factor with constraints in Quarkonia

- discarding all Replicas that yielded unphysical $d\sigma/dy < 0$
→ around half of the Replicas remained.

result set	<i>before</i> re-weighting	<i>after</i> re-weighting
$\sqrt{s} = 7 \text{ TeV} \ \& \ y = 0$	0.2 ± 0.2	0.4 ± 0.1
$\sqrt{s} = 7 \text{ TeV} \ \& \ y = 1$	0.2 ± 0.4	0.4 ± 0.1
$\sqrt{s} = 7 \text{ TeV} \ \& \ y = 2$	0.2 ± 1.1	0.5 ± 0.1
$\sqrt{s} = 14 \text{ TeV} \ \& \ y = 0$	-0.1 ± 0.4	0.3 ± 0.1

K-factor - default scale - updated summary

PDF choice	$\sqrt{s} = 7 \text{ TeV}$			$\sqrt{s} = 14 \text{ TeV}$
	$y = 0$	$y = 1$	$y = 2$	$y = 0$
MRS(G)	1.26	1.27	1.29	1.21
MRS(A')	0.70	0.72	0.76	0.61
NNPDF31sx_nlonllx _as_0118	0.68	0.71	0.80	0.59
CT14nlo_NF3	0.54	0.57	0.65	0.44
NNPDF31sx_nlo _as_0118	0.51	0.52	0.61	0.37
NNPDF31_nlo _as_0118 (re-weighted)	0.4 ± 0.1	0.4 ± 0.1	0.5 ± 0.1	0.3 ± 0.1
NNPDF31_nlo _as_0118 (equal weight)	0.2 ± 0.2	0.2 ± 0.4	0.2 ± 1.1	-0.1 ± 0.4

next step & further constraints on PDFs from Quarkonium Physics

- re-weighted cross-sections are not compatible with s_x and NLL_x

next step & further constraints on PDFs from Quarkonium Physics

- re-weighted cross-sections are not compatible with s_x and NLL_x
→ re-do exercise with s_x and NLL_x

next step & further constraints on PDFs from Quarkonium Physics

- re-weighted cross-sections are not compatible with s_x and NLL_x
→ re-do exercise with s_x and NLL_x
- impose non-negativity using different energies \sqrt{s} and rapidities y

next step & further constraints on PDFs from Quarkonium Physics

- re-weighted cross-sections are not compatible with s_x and NLL_x
→ re-do exercise with s_x and NLL_x
- impose non-negativity using different energies \sqrt{s} and rapidities y
- improve re-weighting by assigning higher weights to Replicas that yield K -factors close to unity rather than sharp 1 and 0 re-weighting

next step & further constraints on PDFs from Quarkonium Physics

- re-weighted cross-sections are not compatible with s_x and NLL_x
→ re-do exercise with s_x and NLL_x
- impose non-negativity using different energies \sqrt{s} and rapidities y
- improve re-weighting by assigning higher weights to Replicas that yield K -factors close to unity rather than sharp 1 and 0 re-weighting
- further constraints for PDFs that we can take from Quarkonium Physics are

next step & further constraints on PDFs from Quarkonium Physics

- re-weighted cross-sections are not compatible with s_x and NLL_x
→ re-do exercise with s_x and NLL_x
- impose non-negativity using different energies \sqrt{s} and rapidities y
- improve re-weighting by assigning higher weights to Replicas that yield K -factors close to unity rather than sharp 1 and 0 re-weighting
- further constraints for PDFs that we can take from Quarkonium Physics are
 - at fixed rapidity, the differential cross-section must increase with \sqrt{s} energy

next step & further constraints on PDFs from Quarkonium Physics

- re-weighted cross-sections are not compatible with s_x and NLL_x
 - re-do exercise with s_x and NLL_x
- impose non-negativity using different energies \sqrt{s} and rapidities y
- improve re-weighting by assigning higher weights to Replicas that yield K -factors close to unity rather than sharp 1 and 0 re-weighting
- further constraints for PDFs that we can take from Quarkonium Physics are
 - at fixed rapidity, the differential cross-section must increase with \sqrt{s} energy
 - at fixed \sqrt{s} energy, the differential cross-section must decrease with increasing rapidity; it must follow the shape of the leading order ($2 \rightarrow 1$ process)

next step & further constraints on PDFs from Quarkonium Physics

- re-weighted cross-sections are not compatible with s_x and NLL_x
 - re-do exercise with s_x and NLL_x
 - impose non-negativity using different energies \sqrt{s} and rapidities y
 - improve re-weighting by assigning higher weights to Replicas that yield K -factors close to unity rather than sharp 1 and 0 re-weighting
 - further constraints for PDFs that we can take from Quarkonium Physics are
 - at fixed rapidity, the differential cross-section must increase with \sqrt{s} energy
 - at fixed \sqrt{s} energy, the differential cross-section must decrease with increasing rapidity; it must follow the shape of the leading order ($2 \rightarrow 1$ process)
- work on-going

$$\sigma \propto H \times \mathcal{C}[f_1^g f_1^g] \quad (6)$$

$$\mathcal{C}[f_1^g f_1^g] = \int \frac{d^2 \vec{b}_T}{(2\pi)^2} e^{i \vec{b}_T \cdot \vec{q}_T} \tilde{f}_1^g(x_1, \vec{b}_T; \zeta, \mu) \tilde{f}_1^g(x_2, \vec{b}_T; \zeta, \mu)$$

$$\tilde{f}_1^{g/A}(x, \vec{b}_T; \zeta, \mu) = \sum_{j=q, \bar{q}, g} \int_x^1 \frac{d\tilde{x}}{\tilde{x}} \tilde{C}_{g/j}(\tilde{x}, \vec{b}_T; \zeta, \mu) f_{j/A}(x/\tilde{x}; \mu)$$

$$\begin{aligned} \tilde{C}_{g/g} = & \delta(1-x) + \frac{\alpha_s}{2\pi} \left[C_A \delta(1-x) \left(-\frac{1}{2} L_T^2 + L_T \ln \frac{\mu^2}{\zeta} - \frac{\pi^2}{12} \right) \right. \\ & \left. - L_T \left(P_{g/g} - \delta(1-x) \frac{\beta_0}{2} \right) \right] \end{aligned}$$

$$\tilde{C}_{g/q} = \frac{\alpha_s}{2\pi} [-L_T P_{g/q} + C_{FX}]$$

$$L_T = \ln \frac{\mu^2 b_T^2}{4e^{-2\gamma_E}}$$

(7)

TMD vs. collinear factorisation

- TMD factorisation is more universal than collinear factorisation

TMD vs. collinear factorisation

- TMD factorisation is more universal than collinear factorisation
 - leading-order process plus virtual corrections are factorised into hard part H (*process-dependent*)

TMD vs. collinear factorisation

- TMD factorisation is more universal than collinear factorisation
 - leading-order process plus virtual corrections are factorised into hard part H (*process-dependent*)
 - real and mixed real-virtual corrections are included inside the TMDPDFs (*process-independent*)

TMD vs. collinear factorisation

- TMD factorisation is more universal than collinear factorisation
 - leading-order process plus virtual corrections are factorised into hard part H (*process-dependent*)
 - real and mixed real-virtual corrections are included inside the TMDPDFs (*process-independent*)
- with positivity constraint $d\sigma/dy > 0$, we have that $\mathcal{C}[f_1^g f_1^g] > 0$ always (universal property)!

TMD vs. collinear factorisation

- TMD factorisation is more universal than collinear factorisation
 - leading-order process plus virtual corrections are factorised into hard part H (*process-dependent*)
 - real and mixed real-virtual corrections are included inside the TMDPDFs (*process-independent*)
- with positivity constraint $d\sigma/dy > 0$, we have that $\mathcal{C}[f_1^g f_1^g] > 0$ always (universal property)!
 - however we encounter at η_c scales, that $\mathcal{C}[f_1^g f_1^g] < 0$

TMD vs. collinear factorisation

- TMD factorisation is more universal than collinear factorisation
 - leading-order process plus virtual corrections are factorised into hard part H (*process-dependent*)
 - real and mixed real-virtual corrections are included inside the TMDPDFs (*process-independent*)
 - with positivity constraint $d\sigma/dy > 0$, we have that $\mathcal{C}[f_1^g f_1^g] > 0$ always (universal property)!
 - however we encounter at η_c scales, that $\mathcal{C}[f_1^g f_1^g] < 0$
- constrain PDFs such that $\mathcal{C}[f_1^g f_1^g] > 0$ at η_c scales

TMD vs. collinear factorisation

- TMD factorisation is more universal than collinear factorisation
 - leading-order process plus virtual corrections are factorised into hard part H (*process-dependent*)
 - real and mixed real-virtual corrections are included inside the TMDPDFs (*process-independent*)
- with positivity constraint $d\sigma/dy > 0$, we have that $\mathcal{C}[f_1^g f_1^g] > 0$ always (universal property)!
 - however we encounter at η_c scales, that $\mathcal{C}[f_1^g f_1^g] < 0$
→ constrain PDFs such that $\mathcal{C}[f_1^g f_1^g] > 0$ at η_c scales
- re-weighting PDFs with similar criteria

TMD vs. collinear factorisation

- TMD factorisation is more universal than collinear factorisation
 - leading-order process plus virtual corrections are factorised into hard part H (*process-dependent*)
 - real and mixed real-virtual corrections are included inside the TMDPDFs (*process-independent*)
- with positivity constraint $d\sigma/dy > 0$, we have that $\mathcal{C}[f_1^g f_1^g] > 0$ always (universal property)!
 - however we encounter at η_c scales, that $\mathcal{C}[f_1^g f_1^g] < 0$
→ constrain PDFs such that $\mathcal{C}[f_1^g f_1^g] > 0$ at η_c scales
- re-weighting PDFs with similar criteria
- if the re-weighted Replicas obtained by imposing $d\sigma/dy > 0$ (+ good shape behaviour) in collinear factorisation more or less coincide with $\mathcal{C}[f_1^g f_1^g]$, this would mean that we are on the right track to use quarkonium as quantitative gluon probes

TMD vs. collinear factorisation

- TMD factorisation is more universal than collinear factorisation
 - leading-order process plus virtual corrections are factorised into hard part H (*process-dependent*)
 - real and mixed real-virtual corrections are included inside the TMDPDFs (*process-independent*)
- with positivity constraint $d\sigma/dy > 0$, we have that $\mathcal{C}[f_1^g f_1^g] > 0$ always (universal property)!
 - however we encounter at η_c scales, that $\mathcal{C}[f_1^g f_1^g] < 0$
→ constrain PDFs such that $\mathcal{C}[f_1^g f_1^g] > 0$ at η_c scales
- re-weighting PDFs with similar criteria
- if the re-weighted Replicas obtained by imposing $d\sigma/dy > 0$ (+ good shape behaviour) in collinear factorisation more or less coincide with $\mathcal{C}[f_1^g f_1^g]$, this would mean that we are on the right track to use quarkonium as quantitative gluon probes
→ work on-going

Backup

shape of rapidity differential at LO - CT14nlo_NF3

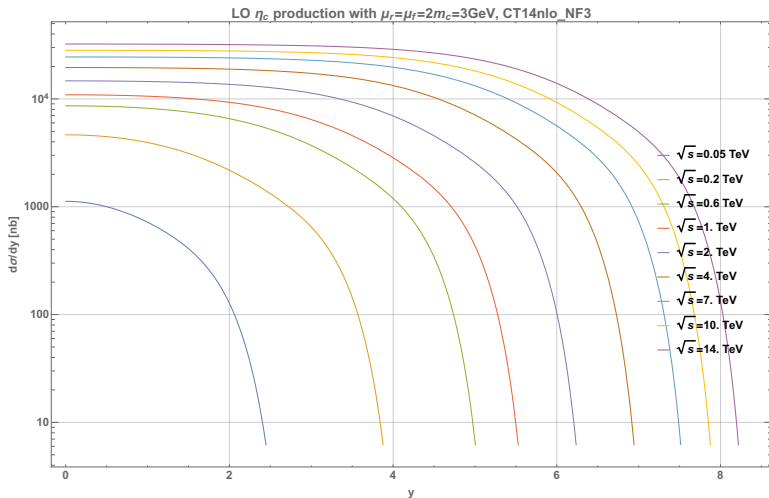


Figure: rapidity differential cross-section at LO for different energies, default scale choice, CT14nlo_NF3

shape of rapidity differential at NLO - CT14nlo_NF3, def.

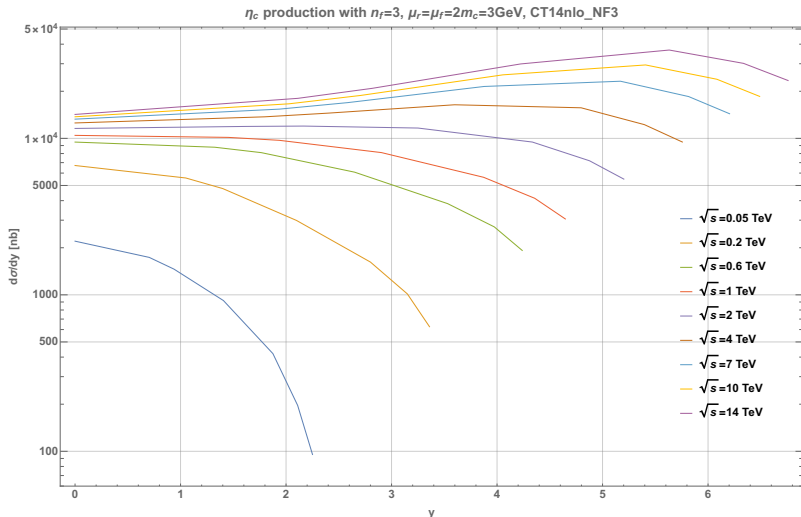


Figure: rapidity differential cross-section at NLO for different energies, default scale choice, CT14nlo_NF3

shape of rapidity differential at NLO - CT14nlo_NF3, alt.

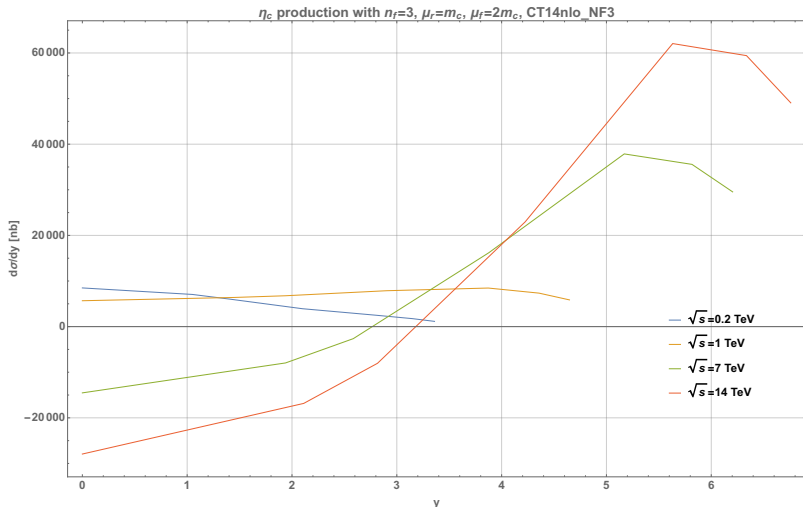


Figure: rapidity differential cross-section at NLO for different energies, alternative scale choice, CT14nlo_NF3

shape of rapidity differential at NLO - NNPDF31sx_nlo_as_0118

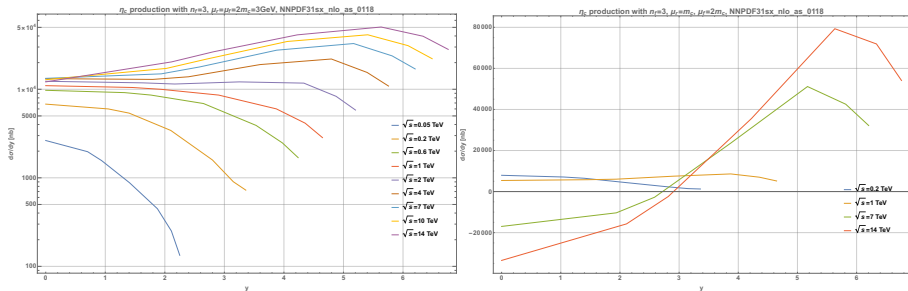


Figure: rapidity differential cross-section at NLO for different energies, default/alternative scale choice, NNPDF31sx_nlo_as_0118

shape of rapidity differential at NLO - NNPDF31sx_nlonlx_as_0118

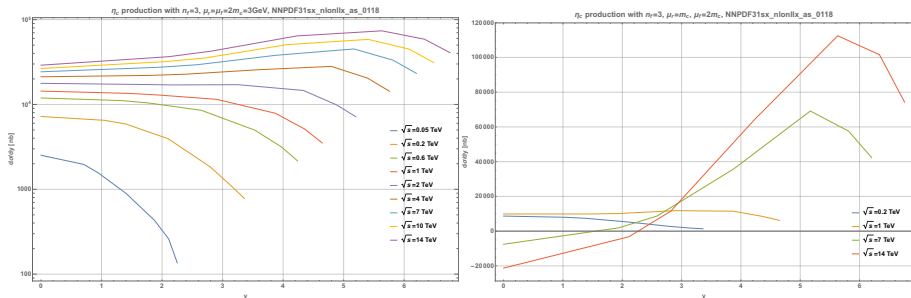


Figure: rapidity differential cross-section at NLO for different energies, default/alternative scale choice, NNPDF31sx_nlonlx_as_0118

- **Colour-Evaporation Model**
 - quark and anti-quark colours are summed up at amplitude squared level (evaporation)
 - no spin-projection
- **Colour-Octet Model**
 - quark and anti-quark pair are in color-octet state
 - heavy quark spins projected on final bound state
 - higher Fock states in NRQCD, higher v -order
- **Colour-Singlet Model**
 - quark and anti-quark pair are in color-singlet state
 - heavy quark spins projected on final bound state
 - leading Fock state in NRQCD

gluon-gluon channel

$$\begin{aligned}
 \hat{\sigma}_{gg}(s, \hat{s}, \mu_R, \mu_F) = & \frac{\alpha_s^2(\mu_R)\pi^2}{96m_c^5} |R(0)|^2 \delta(1-z) \\
 & + \frac{\alpha_s^3(\mu_R)\pi}{1152m_c^5} |R(0)|^2 \left[\left(-44 + 7\pi^2 + 54 \log\left(\frac{\mu_R^2}{\mu_F^2}\right) \right. \right. \\
 & + 72 \log\left(1 - \frac{4m_c^2}{s}\right) \left(\log\left(1 - \frac{4m_c^2}{s}\right) - \log\left(\frac{\mu_F^2}{4m_c^2}\right) \right) \left. \right) \delta(1-z) \\
 & + 6 \left(24 \left(\frac{\log(1-z)}{1-z} \right)_\rho (1 - (1-z)z)^2 \right. \\
 & + 12 \left(\frac{1}{1-z} \right)_\rho \frac{\log(z)}{(1-z)(1+z)^3} (1 - z^2 (5 + z(2 + z + 3z^3 + 2z^4))) \\
 & - \left(\frac{1}{1-z} \right)_\rho \frac{1}{(1+z)^2} (12 + z^2 (23 + z(24 + 2z + 11z^3))) \\
 & \left. \left. + 12(1+z^3)^2 \log\left(\frac{z\mu_F^2}{4m_c^2}\right) \right) \right], \text{ where } z = 4m_c^2/\hat{s} \text{ and } \rho = 4m_c^2/s
 \end{aligned}$$

(8)

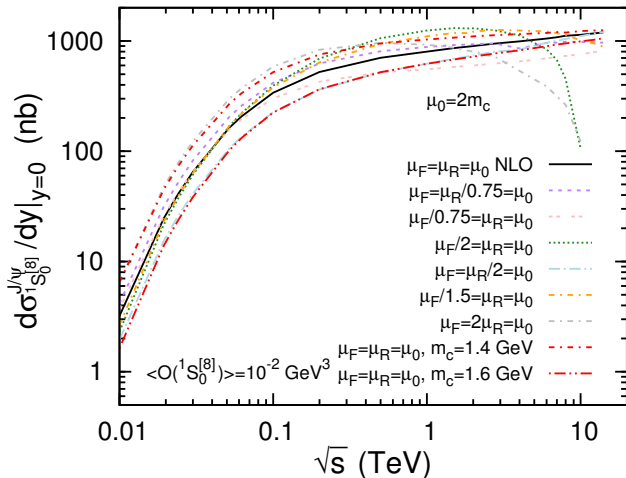
quark-antiquark channel

$$\hat{\sigma}_{q\bar{q}}(\hat{s}, \mu_R) = \frac{16\alpha_s^3(\mu_R)\pi}{81m_c} |R(0)|^2 \frac{(\hat{s} - 4m_c^2)}{\hat{s}^3} \quad (9)$$

quark-gluon channel

$$\begin{aligned} \hat{\sigma}_{qg}(\hat{s}, \mu_R, \mu_F) = & \frac{\alpha_s^3(\mu_R)\pi}{72m_c^5\hat{s}^2} |R(0)|^2 (8m_c^4 + 4m_c^2\hat{s} - \hat{s}^2 \\ & + 2(8m_c^4 - 4m_c^2\hat{s} + \hat{s}^2) \log\left(1 - \frac{4m_c^2}{\hat{s}}\right) \\ & + \hat{s}(-4m_c^2 + \hat{s}) \log\left(\frac{4m_c^2}{\hat{s}}\right) \\ & - (8m_c^4 - 4m_c^2\hat{s} + \hat{s}^2) \log\left(\frac{\mu_F^2}{\hat{s}}\right) \end{aligned} \quad (10)$$

problem of negative cross-sections - J/ψ , $^1S_0^{[8]}$ at NLO



comparison of J/ψ $^1S_0^{[8]}$ differential cross-section at NLO with different choices of μ_R and μ_F with CTEQ6M [Y. Feng, J.-P. Lansberg, J.X. Wang, Eur.Phys.J. C75 (2015)]

- let's define $z = M^2/\hat{s}$ and $\tau_0 = M^2/s$
- LO partonic cross-section and virtual corrections ($2 \rightarrow 1$ process) have $\delta(1 - z)$ function while real corrections ($2 \rightarrow 2$) are complicated functions of z
- negative contributions come from real corrections which have interference terms
- idea is to use simple toy-models for gluon PDFs and convolute with partonic cross-section; different z -terms will contribute differently at hadronic level

	$xg(x) \rightarrow 1$	$xg(x) \rightarrow 1/\sqrt{x}$
$\hat{\sigma}_{gg}(z, M^2)$	$\sigma_{pp}(\tau_0, M^2) \xrightarrow{\tau_0 \rightarrow 0}$	
$\delta(1-z)$	$\ln\left(\frac{1}{\tau_0}\right)$	$\frac{1}{\sqrt{\tau_0}} \ln\left(\frac{1}{\tau_0}\right)$
z^k	$\frac{1}{k} \ln\left(\frac{1}{\tau_0}\right)$	$\frac{2}{(2k+1)\sqrt{\tau_0}} \ln\left(\frac{1}{\tau_0}\right)$
1	$\frac{1}{2} \ln^2\left(\frac{1}{\tau_0}\right)$	$\frac{2}{\sqrt{\tau_0}} \ln\left(\frac{1}{\tau_0}\right)$
$\ln^k\left(\frac{1}{z}\right)$	$\frac{1}{(k+1)(k+2)} \ln^{k+2}\left(\frac{1}{\tau_0}\right)$	$\frac{k! 2^{k+1}}{\sqrt{\tau_0}} \ln\left(\frac{1}{\tau_0}\right)$

Asymptotic ($\tau_0 = M^2/s \rightarrow 0$) behaviour of the proton-proton or proton-antiproton cross section for various forms of the gluon-gluon subprocess ($z = M^2/\hat{s} = \tau_0/\tau$) and two extreme choices of the gluon distribution function. Taken from G. Schuler, Review, 1994

toy model $g(x) = 1/x$: real corrections dominate at high energies;
 toy model $g(x) = 1/x^{1.5}$: all contributions have same energy scaling

partonic cross-section away from threshold, $z \rightarrow 0$

$$\lim_{z \rightarrow 0} \hat{\sigma}_{gg} = \frac{\alpha_s^3(\mu)\pi}{16m_c^5} |R(0)|^2 \left(\log \left(\frac{4m_c^2}{\mu_F^2} \right) - 1 \right), \quad (11)$$

$$\lim_{z \rightarrow 0} \hat{\sigma}_{q\bar{q}} = 0, \quad (12)$$

$$\lim_{z \rightarrow 0} \hat{\sigma}_{qg} = \frac{\alpha_s^3(\mu)\pi}{72m_c^5} |R(0)|^2 \left(\log \left(\frac{4m_c^2}{\mu_F^2} \right) - 1 \right) \quad (13)$$

partonic cross-section away from threshold, $z \rightarrow 0$

- $\mu_F = m_c$

$$\lim_{z \rightarrow 0} \hat{\sigma}_{gg} = \frac{\alpha_s^3(\mu)\pi}{16m_c^5} |R(0)|^2 (\log(4) - 1) = 0.2 * \hat{\sigma}_{gg,LO}, \quad (14)$$

- $\mu_F = 2m_c$

$$\lim_{z \rightarrow 0} \hat{\sigma}_{gg} = \frac{\alpha_s^3(\mu)\pi}{16m_c^5} |R(0)|^2 (-1) = -0.5 * \hat{\sigma}_{gg,LO}, \quad (15)$$

- toy model 1 PDF with $f_{g/p}(x) = 1/x$
 - dependence of hadronic cross-section on μ_F
 - for $\mu_F > m_c$, hadronic cross-section is negative
 - for $\mu_F < m_c$, hadronic cross-section is positive
- toy model 2 PDF with $f_{g/p}(x) = 1/x^{1.5}$
 - weak dependence of hadronic cross-section on μ_F
 - cross-section always positive (independent of choice of μ_F)
- similar behaviour for qg channel at high energies because of same asymptotic limit as in gg channel apart from global factor

- for non-steep PDF choices, the high-energy hadronic limit is governed by the high-energy partonic limit \rightarrow strong dependence on factorisation scale μ_F
- some values for C_J :
 - $C_J = 1$ for pseudo-scalar quarkonia $\eta_{c/b/t}$
 - $C_J = 43/27$ for $\chi_{c/b,0}$
 - $C_J = 53/36$ for $\chi_{c/b,2}$
 - $C_J = 11/12 + \log z$ for Higgs (in infinite-top quark mass limit)
- as an aside note, ratio between qg and gg channel in high-energy partonic limit is process-independent (same for Quarkonia and Higgs Physics)

$$\lim_{z \rightarrow 0} \frac{\hat{\sigma}_{qg}}{\hat{\sigma}_{gg}} = \frac{C_F}{2C_A} = \frac{2}{9} \quad (16)$$